IEEE Access
Multidisciplinary | Rapid Review | Open Access Journal

Received October 23, 2019, accepted October 31, 2019, date of publication November 15, 2019, date of current version December 3, 2019.

Digital Object Identifier 10.1109/ACCESS.2019.2953796

Wide Color Gamut Autostereoscopic 2D–3D Switchable Display Based on Dynamic Subpixel Arrangement

BIN XU, XUELING LI, AND YUANQING WANG
School of Electronic Science and Engineering, Nanjing University, Nanjing 210023, China
Corresponding author: Yuanqing Wang (yqwang@nju.edu.cn)

This work was supported in part by the National Key Research and Development Plan under Grant 2016YFB0401503, and in part by the Research and Development Plan of Jiangsu Science and Technology Department under Grant BE2016173.

ABSTRACT This paper is a report on the mathematical analysis and working principle of a wide color gamut autostereoscopic 2D-3D switchable display based on the dynamic subpixel arrangement method. The display prototype discussed in the paper has three major distinctions. First, the use of dynamic subpixel arrangement method and eye-tracking system has improved its performances in the resolution, crosstalk and 2D/3D switching statistics. Second, a design of Quantum-Dot-Polymer (QDP) film and optical layer combined backlight has enhanced its viewing angle and color gamut. Third, the application of parallel computing to the dynamic subpixel arrangement method has improved its real-time performance. Base on observation from finished fabrication and experiment, this prototype has already demonstrated noticeable enhancement in terms of color gamut expansion-reaching 77.98% according to ITU-R Recommendation BT.2020 (Rec.2020), and crosstalk reduction-with the minimum crosstalk rate at nearly 6%. Close comparison with two other commercial 3D displays (BENQ XL2707-B and View Sonic VX2268WM) are also presented in the paper for sufficiency.

INDEX TERMS 3-D display, dynamic subpixel arrangement, quantum dot, color gamut.

I. INTRODUCTION

Since its creation, three-dimensional (3D) display has been attracting uninterrupted attention from academia and businesses. It is believed that, compared with traditional displays [1], 3D devices offer better viewing experience with depth information.

Among a range of 3D displays, typical stereoscopic ones equipped with auxiliary glasses (e.g. active shutter glasses [2], [3] or polarized glasses [4]–[6]) are frequently chosen for relatively low crosstalk rate. Modern active shutter 3D glasses consist of two individual voltage-activated shutter lenses. The shutter lens is made by liquid crystal. As those transparent lenses would turn opaque at a voltage to block the view, when a vertical synchronization signal aligned with screen refresh rate appropriately controls the alternate voltage, 3D display could be delivered through. Polarized glasses are commonly chosen by 3D cinemas. When they are equipped with silver or aluminized screens, polarization could be well reserved and the crosstalk is quite low.

However, limitations as inconvenience of wearing glasses and noticeable brightness loss are hindering stereoscopy's development especially with the rise of the autostereoscopic display researches. Spatial-multiplexed displays which utilize lenticular lens [7]–[9] and parallax barrier [10]–[12] are examples already in wide use. Although, these solutions are still faced with inevitable compromise between the viewpoint number and the perceived resolution, narrow viewing angle, crosstalk and incompatible data format. It still could be argued that, the autostereoscopic display technology will be the next-generation technology.

Justification of this argument and some inspiring ideas could already be drawn from former studies: 3D image quality decline of autostereoscopic displays caused by crosstalk and resolution loss could be solved by redesigning subpixel shapes [13]; while directional backlight solution [14]–[17], which enables separation of the left-eye and right-eye image, when combined with eye tracking system could largely

The associate editor coordinating the review of this manuscript and approving it for publication was You Yang.

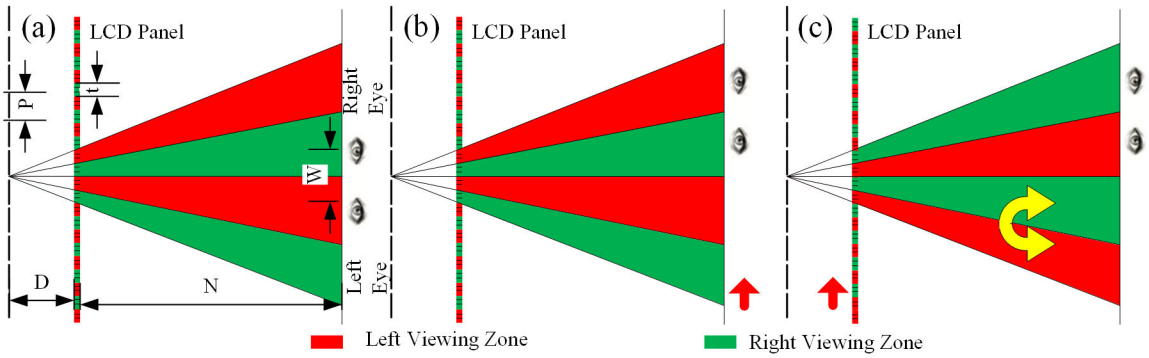

FIGURE 1. (a) Principle of parallax barrier illumination autostereoscopic display. (b) Pseudo-Stereo phenomenon. (c) Change subpixel arrangement order to form correct exit pupil when eyes are at new position.

overcome resolution and crosstalk issues from multiple viewer positions. By now, crosstalk rate of those autostereoscopic displays has been reduced to match stereoscopic ones with auxiliary glasses. Those improvements have laid a solid foundation for wide future application of directional backlight. Conform with those research focuses within the field, this study is intended to further relevant studies on 3D display quality of autostereoscopic devices, including resolution, crosstalk and brightness, and discuss the issues about color gamut [18]–[20] based on our prototype, an updated version of present binocular eye-tracking display.

In the ordinary eye-tracking displays, two images (Left image and Right image) with small parallax are used to produce exit pupils. But these stationary and discontinuous exit pupils, whose distribution in vision is determined by parallax barrier or lenticular lens, will lead to reverse display of two stereo images when a viewer is not on the ideal viewing position.

In 3D display with continuous motion parallax and depth range, in order to tackle the similar issue, we introduce the dynamic subpixel arrangement method to improve viewer experience in motion. i.e. when the viewer moves, the exit pupils will follow the eyes of the viewer by changing the arrangement of the subpixels. While processing the changing eye position information tracked by eye-tracking system, this precise mechanical structure could provide high-resolution, low crosstalk 3D images as the viewer moves in a wide viewing range in Z-direction.

In order to realize the maximum pixel resource of its liquid crystal display (LCD) panel, this prototype adds an optical layer to distribute the light of individual pixel evenly. And data for each pixel is processed independently by parallel computing.

Other features of our solution include: the cost-efficiency design, simpler algorithm, available high performance in 2D mode, and the great commercialization potential. First, compared with the complex equipment used in integral imaging [21], [22], light field [23]–[24], holography [25], [26], or other techniques, our prototype appears more economic and efficient, since existing commercial 2D displays as personal monitors, tablets and smartphones could be swiftly updated into a 2D-3D switchable one according to our design. Second, in terms of the algorithm used in different systems, prior algorithms for integral imaging, light field, holography are not simplified enough to provide stable real-time performance, whereas our system has introduced parallel computing to streamline the algorithm, and bring forth a better real-time performance. Third, this display is a 2D/3D switchable one. It could be used in 2D mode at the physical resolution of the LCD panel. Fourth, as the front-facing camera has been designed into most commercial devices in the fields of personal monitors, tablets and smartphones, by which eye-tracking algorithm within our prototype could be easily realized thereupon. This refers to a huge applicability in future.

Based on experimental studies, there are three major discoveries of our prototype. First, the dynamic subpixel arrangement method as an updated reconstruction strategy could reduce crosstalk effects in real-time 3D display. Second, improving real-time performance of the motion parallax could optimize 3D display experience viewed from different positions. Third, the application of Quantum-Dot (QD) material could further enhance the color expression of display by extending its color gamut.

II. SYSTEM CONFIGURARION AND OPERATION PRINCIPLE

A. SYSTEM DESCRIPTION

This system is an autostereoscopic display based on the principle of parallax barrier illumination. It mainly consists of a QD backlight, a parallax barrier and a dynamic subpixel arrangement module. As viewing position of the viewer changes, continuous viewing zones will be formed and adjusted accordingly.

Fig. 1(a) is a simple despcription of the dislplay. P is the period of the grating, and t LCD pixel pitch. D refers to the distance between the LCD panel and the grating. N is the viewing distance between the viewer and the display. W is the distance between adjacent left and right exit pupil, about 60mm. $\beta = \mathrm{W/t} - 1$ is defined as 3D magnification factor.

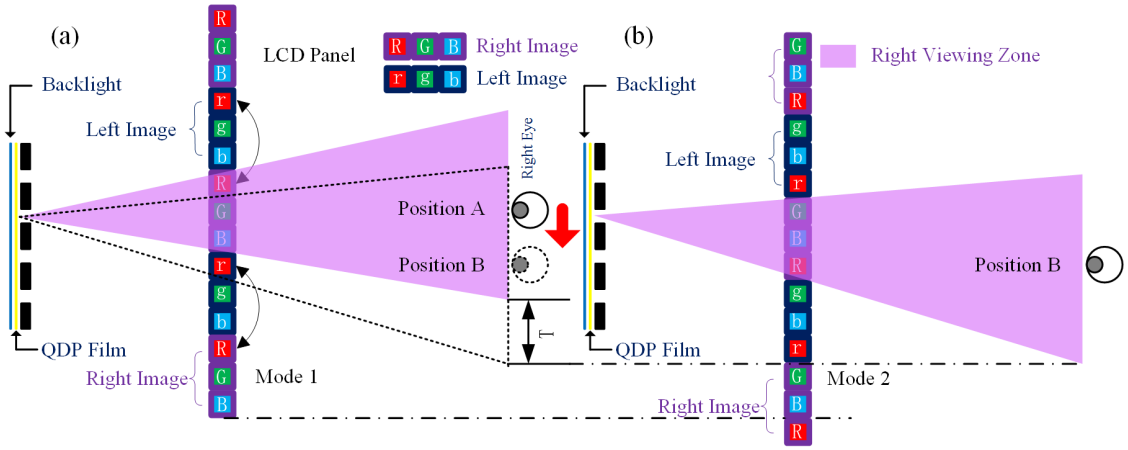

FIGURE 2. Diagram of Dynamic Subpixel Arrangement (a) Mode 1 of subpixel arrangement (b) Mode 2 of subpixel arrangement.

As shown in Fig. 1(a), the 3D display based on parallax barrier has an inherent disadvantage: the exit pupil at best viewing distance is stationary. Viewer could perceive correct 3D images only if their two eyes are in the correct viewing zone. i.e. when the left eye moves into the R region and the right eye moves into the L region, Pseudo-Stereo would emerge, as shown in Fig. 1(b). Theoretically, as the L region and R region at the best viewing position have the same width, the rate of Pseudo-Stereo appearance is 50%.

However, as Fig. 1(c) illustrates, when human eyes remain stable, it's possible to move fused image in either direction to where the correct images of two eyes recovered. Given that every individual pixel is composed of "RGB" (Red, Green and Blue) sub-pixels, and correct image display only relies on information integrity regardless of specific order. Pseudo-stereo phenomenon could be avoided if the sub-pixel arrangement order could be adjusted in accordance with the eye position.

Assuming that the human eye does not move at this time and the fused image moves in one direction, the original position of the left image becomes the right image and the original position of the right image becomes the left image, as shown in Fig. 1(c). After adjustment, the result is that the left eye sees the left image and the right eye sees the right image.

For example, before crosstalk occurs, the fused image could move a single sub-pixel in one direction, changing the arrangement of the subpixels from "RGB" to "BRG", without compromising the information integrity of the whole pixel unit.

A more specific illustration is shown in Fig. 2.(a). Capitalized letters "RGB" represent the right image, and "rgb" represents the left eye's. At position A, the light purple area stands for the correct exit pupil of "RGB" (Mode 1) with no crosstalk. But when the right eye moves to the position B, two-thirds of the right image ("GB") and one-third of the left image ("r"), are seen simultaneously within the dotted-lined area, causing 1/3 crosstalk.

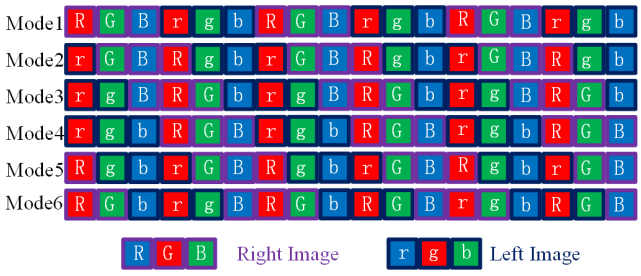

FIGURE 3. 6 modes of dynamic subpixel rearrangement.

In order to avoid this problem, the red subpixel ("r") is substituted by "R" to re-display the correct right eye image (Mode 2), as shown in Fig. 2(b). The order of subpixels is now changed to "GBR". Compared with Mode 1, the whole image moves 1/3 pixel, and the movement of the exit pupil is T = W/6. Corrispondingly, other subpixel arrangement modes could be formed when the eye moves to new postion. In Fig. 3 and Fig. 4, all six possible display modes are listed in table and illustated repectively.

To be noticed, both clored regions representing correct exit pupils are divided into three parts to better track the movement of eyes with accuracy, as shown in Fig. 4. Anytime viewer's two eyes are dectected out of the central units (R2 and L2), the subpixel arrangement would soon adapt to prevent Pseudo-Stereo effects.

B. RELATIONSHIP BETWEEN EYE POSITION AND SUBPIXEL ARRANGEMENT MODE

As mentioned above, using six subpixel arrangement modes could deliver correct exit pupils regardless of the eyes' position. It is necessary to analyze how subpixel arrangement mode would work specifically when eye position changes.

In the experiment discussed in this section, Field Programmable Gate Array (FPGA) is used to receive the high-speed video signal and realize the mode switching algorithm.

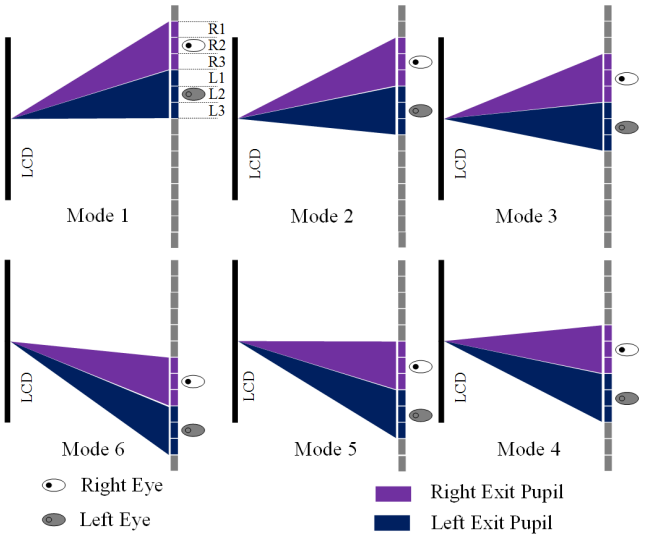

FIGURE 4. The viewer's eye movement and the switching of exit pupil.

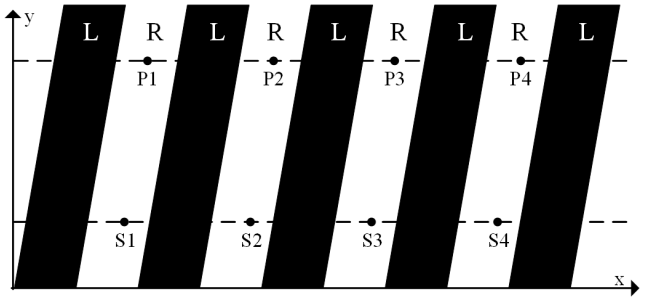

FIGURE 5. The image captured by camera which is fixed in front of the prototype.

Parallel computing method is used for strict control of time delay.

When experiment begins, a white screen is erected in front of the display at the best viewing position, and two black horizontal lines are drawn in the middle to position the camera screen. Then images fused by pure black and white are played for tests and measurements. But in the left-eye view only pure black images would be seen, and in the right-eye view, only pure white images.

In this setting, exit pupil parameters are determined. When test image 1 (Mode 1) is played, periodic black and white stripes appear on the white screen. Central positions (P_1-P_4) of white stripes of several cycles could be marked on the above horizontal lines; then as test image 2 (Mode 2) played, another set of central positions (S_1-S_4) could be marked, as shown in lower part of Fig. 5.

The coordinates of P_1, P_2, P_3, P_4, S_1, S_2, S_3, S_4 can be expressed as $P(x_i, y_i)$, $i \in [1,2,3,4]$, $S(x_j, y_j)$, $j \in [5,6,7,8]$. The width of the exit pupil (P) can be calculated by Eqs. (1).

$$P = \frac{1}{6}\left(\sum_{i=2}^{4}(x_i - x_{i-1}) + \sum_{i=6}^{8}(x_i - x_{i-1})\right) \tag{1}$$

FIGURE 6. (a) The blue LEDs used in this system. (b)The parallax barrier, QDP film and diffusion film.

Given that a cycle consists of six subpixel arrangement modes, and the distance between each exit pupil center is $p = P/6$.

Then the slope of those stripes could be calculated by Eqs. (3) and Eqs. (4).

$$k = \frac{dx}{dy} \tag{2}$$

$$dx = \frac{1}{4}\sum_{i=5}^{8}(x_i - x_{i-4}) \tag{3}$$

$$dy = \frac{1}{4}\sum_{i=5}^{8}(y_i - y_{i-4}) \tag{4}$$

Assume that P_2 (x_2, y_2) is selected as the reference point, i.e. when mode of P_2 is set as 2 ($m = 2$). The relationship between mode and coordinates of that viewing point could be written as:

$$M = (x_2, y_2, m, p, k, \lambda) \tag{5}$$

Here, parameter λ is set to indicate the moving direction of the exit pupil. If the central point of exit pupil moves right, λ is set as 1. If it moves left, λ is set as -1.

Thereby, if the viewer's eyes position detected by the eye tracking system is Q (x_0, y_0), the distance between Q and the reference point P_2 could be calculated in Eqs. (6).

$$d = k\,(y_0 - y) + (x - x_0) \tag{6}$$

The width of the exit pupil is P and the pattern distribution is periodic.

Last, as parameter d and d' have the same subpixel arrangement mode (as shown in Eqs. (7)), the corresponding mode (Q_m) of position Q could be figured out with Eqs. (8) and Eqs. (9) together.

$$d' = d\%P \tag{7}$$

$$\nabla_m = \begin{cases} 0, \left|d'\right| \le \dfrac{p}{2} \\ \left\lfloor \dfrac{1}{p}\left|d' - \dfrac{d'}{|d'|}\cdot\dfrac{p}{2}\right| \right\rfloor + 1, \left|d'\right| > \dfrac{p}{2} \end{cases} \tag{8}$$

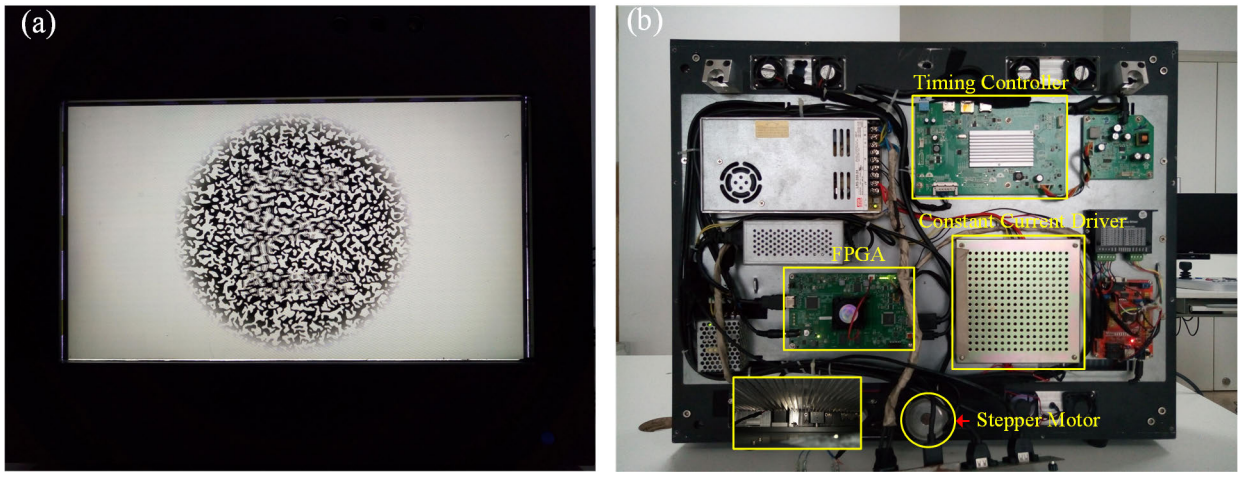

FIGURE 7. Prototype of our display. (a) The front view of our prototype. (b)The rear view of our prototype.

$\nabla_m \in [0,5]$. The mode of Q can be defined as

$$Q_m = \mathrm{m} + \frac{d}{|d'|}\lambda\nabla_m \tag{9}$$

C. THE PRINCIPLE OF VIEWING DISTANCE CONTROL

In theory, the relationship between N (the best viewing distance) and D (the distance between parallax barrier and LCD panel) can be described as $N = \beta * D$. β stands for the magnification factor.

Thus, the best viewing distance (between exit pupil and the display) is pre-determined by the distance between the parallax barrier and the LCD panel.

But this prototype includes a special design. It could adjust the distance between the parallx barrier and the LCD panel to form the most appropriate exit pupil at any viewing point within the Z-direction viewing range. The best viewing distance then becomes a controllable dynamic factor.

D. THE PRINCIPLE OF 2D/3D SWITCHING

In our prototype, the function of 2D/3D switching is based on the use of Polymer Dispersed Liquid Crystal (PDLC) [27].

It is assumed that, in 2D mode, the PDLC operating as an ordinary diffusion film, would turn slit light source into diffuse one; while the prototype is in 3D mode, the PDLC would turn to be transparent at voltage signals. Several experiments are carried out to justify this design's feasibilty[28].

III. PROTOTYPE SETUP

Table. 1. provides basic information of the LCD panel used in our design.

Fig. 6(a) is an aluminum substrate orderly dotted with blue LEDs. Fig. 6(b) shows the assemble order of the parallax barrier, the QDP film and the diffusion film.

The width (W) of the exit pupil is set as 60mm, which is equal to the distance between viewer's two eyes. Parameter P is set as 137.25um.

TABLE 1. Display characteristics.

Screen Diagonal	23.8″
Pixel Pitch(mm)	0.2715 (H) x 0.2715 (V)
Display Colors	1.07G colors
Pixel H*V	3840(RGB)*2160
Frame Rate	60Hz
Pixel Arrangement	RGB vertical stripe

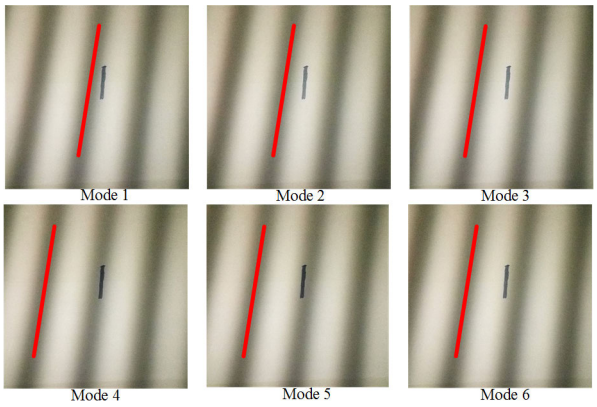

FIGURE 8. The movement of the exit pupil.

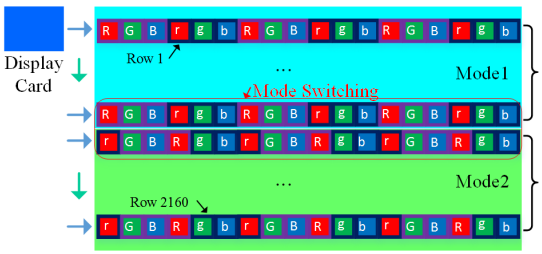

FIGURE 9. The principle of the mode switching.

Shown in Fig. 7(b), our prototype is composed of a timing controller, a FPGA, a constant current driver and a stepper motor. The FPGA is used for dynamic subpixel arrangement

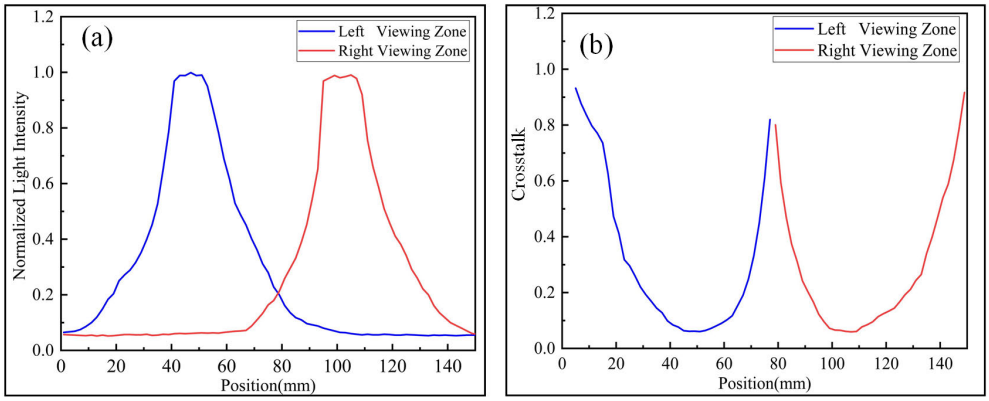

FIGURE 10. (a) Normalized light intensity of the viewing zones. (b) The crosstalk in different position.

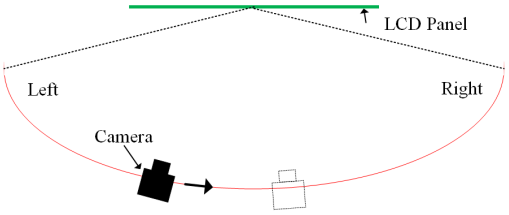

FIGURE 11. Schematic diagram of the measuring device.

method, the stepper motor for adjusting the distance between the parallax barrier and the LCD panel. The arrangement of the stepper motor can be seen in the enlarged picture.

IV. EXPERIMENT AND RESULT

A. THE EVALUATION OF VIEWING ZONE SWITCHING

Fig. 8 shows all exit pupils in 6 modes projected at the best viewing distance on the white screen. Compared with the short black line, the exit pupil will move W/3 (20mm) at each mode switching, and 120mm in a complete circle.

As illustrated in Fig. 9, the display card sends the image data by row. With a 3840(RGB)∗2160 resolution and 60Hz (16.66ms) frame rate (see Table. 1.), the transmission time for each row will be 7.72us (16.66ms/2160).

Cluster communication port (COM) is in charge of transmitting the viewer's eye position data from the eye-tracking system to the FPGA. The baud rate of the COM port is set as 115200 bps. The frame rate of the camera is 60Hz and its resolution is 640∗480.

This design means that, when the data of a new eye position is generated, corresponding mode switching could be completed in 7.72us by the FPGA.

B. THE EVALUATION OF CROSSTALK

As mentioned from the beginning part, viewing experience of 3D displays is greatly influenced by the

FIGURE 12. (a)-(l) Perspectives observed from left to right.

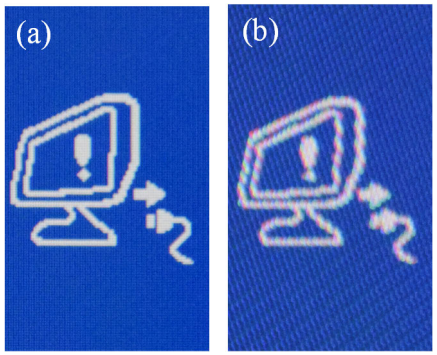

FIGURE 13. (a) Picture displayed in 2D mode. (b) Picture displayed in 3D mode.

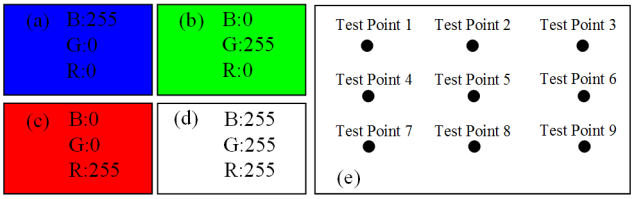

FIGURE 14. (a) The pure blue image for the test. (b) The pure green image for the test. (c) The pure red image for the test. (d) The pure white image for the test. (e) Nine measuring points.

crosstalk [29]–[31]. To measure 3D display quality, unexpected rays ratio is an important factor.

Crosstalk ratio of the nth view zone in N viewing zones [20] could be defined as Eqs. (10).

$$CR_n = \frac{\sum_{j=1,j\neq n}^{N} LightIntensity_{(j)}}{\sum_{j=1}^{N} LightIntensity_{(j)}} \tag{10}$$

The display color analyzer (CA-310: manufactured by KONIC MINOLTA) is used to measure the light distribution of the exit pupil at the viewing distance. Normalized light intensity is shown in Fig. 10(a). The blue line represents the light distribution of the left viewing zone for the left eye and the red line represents the light distribution of the right viewing zone for the right eye. The distance between the left and right viewing zone is about 60mm, which is equivalent to the distance between human eyes. As shown in Fig. 10(b), calculated minimal crosstalk is about 6%, according to Eqs. (10).

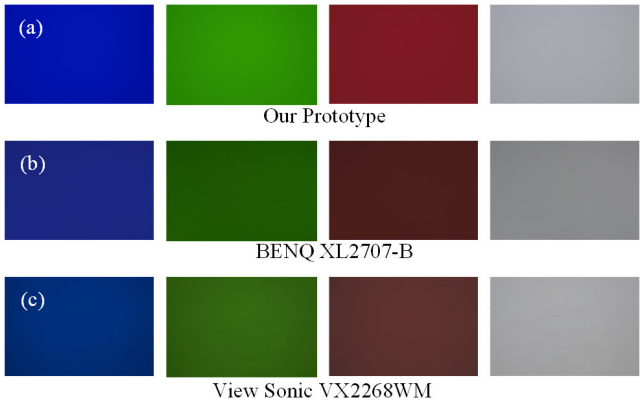

FIGURE 15. (a) When the different test images are displayed by our prototype, the photos are recorded. (b) When the different test images are displayed by BENQ XL2707-B, the photos are recorded. (c) When the different test images are displayed by View Sonic VX2268WM, the photos are recorded.

Fig. 11 presents the schematic diagram of a camera serving as a measuring device (Nikon D3300, Exposure parameter: f/2.2, ISO-160, 1/33s) to simulate eye view. Its shootings from 12 perspectives are shown in Fig. 12. One thing to note, parts of the Fig. 12(f) and Fig. 12(g) are magnified for closer observation. We can see the circled parallax difference in between. When the left eye is in the viewing zone as shown in Fig. 12(f) and right eye is in the viewing zone as shown in Fig. 12(g), viewer will enjoy good 3D experience.

C. THE EVALUATION OF 2D/3D SWITCHING

Our prototype is a 2D/3D switchable one. In Fig. 13(a), the image is displayed in 2D mode and the display resolution is equal to the physical resolution (3840∗2160) of the LCD panel. While less than ideal, the display resolution would be reduced to 1920∗1080 in 3D mode, as it shows in Fig. 13(b). Experiment shows that our prototype can be not only used

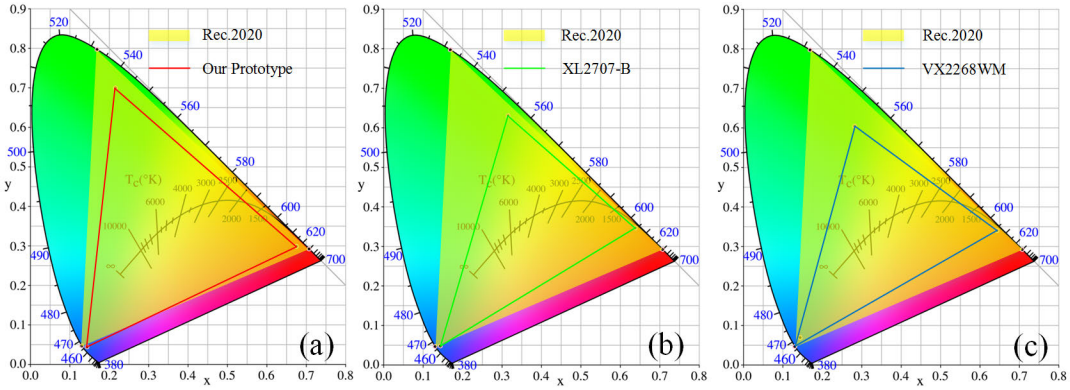

FIGURE 16. The color gamut. (a) The color gamut of our prototype. (b) The color gamut of BENQ XL2707-B. (c) The color gamut of View Sonic VX2268WM.

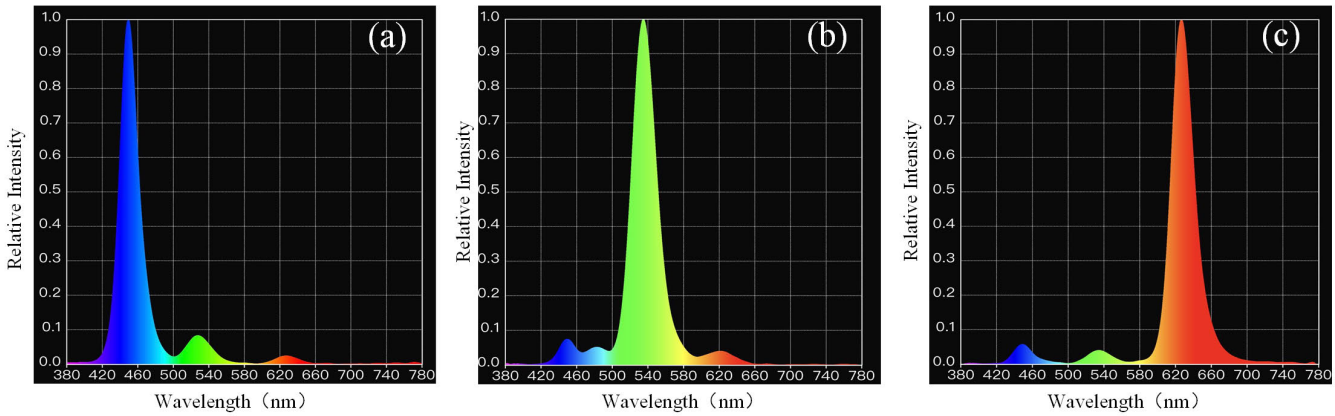

FIGURE 17. Spectrums of the prototype in different test conditions. (a) The spectrum when the LCD is displaying the pure blue image. (b) The spectrum when the LCD is displaying the pure green image. (c) The spectrum when the LCD is displaying the pure red image.

TABLE 2. The recorded coordinates.

		R_x	R_y	G_x	G_y	B_x	B_y
Our Prototype	1	0.6776	0.2981	0.2137	0.6995	0.1439	0.0445
	2	0.6762	0.2984	0.2153	0.7019	0.1431	0.0423
	3	0.6779	0.2997	0.2180	0.7016	0.1432	0.0437
	4	0.6765	0.2980	0.2149	0.6983	0.1438	0.0456
	5	0.6758	0.2985	0.2164	0.7017	0.1436	0.0442
	6	0.6764	0.2992	0.2182	0.7009	0.1434	0.0456
	7	0.6744	0.2982	0.2120	0.6977	0.1439	0.0426
	8	0.6768	0.2989	0.2168	0.7002	0.1434	0.0424
	9	0.6758	0.2988	0.2189	0.6998	0.1438	0.0439
BENQ XL2707-B	1	0.6375	0.3472	0.3172	0.6314	0.1439	0.0482
	2	0.6383	0.3471	0.3163	0.6312	0.1438	0.0483
	3	0.6374	0.3462	0.3154	0.6299	0.1435	0.0478
	4	0.6389	0.3477	0.3177	0.6301	0.1441	0.0482
	5	0.6383	0.3479	0.3172	0.6289	0.1438	0.0474
	6	0.6369	0.3471	0.3167	0.6299	0.1436	0.0472
	7	0.6379	0.3470	0.3162	0.6301	0.1442	0.0490
	8	0.6385	0.3471	0.3158	0.6312	0.1438	0.0481
	9	0.6389	0.3476	0.3168	0.6291	0.1429	0.0479
View Sonic VX2268 WM	1	0.6440	0.3392	0.2809	0.6034	0.1433	0.0677
	2	0.6435	0.3390	0.2809	0.6025	0.1436	0.0677
	3	0.6448	0.3398	0.2829	0.6049	0.1434	0.0696
	4	0.6451	0.3396	0.2822	0.6051	0.1434	0.0693
	5	0.6437	0.3400	0.2823	0.6031	0.1438	0.0691
	6	0.6457	0.3402	0.2841	0.6067	0.1438	0.0722
	7	0.6437	0.3404	0.2821	0.6043	0.1432	0.0685
	8	0.6431	0.3401	0.2825	0.6037	0.1435	0.0686
	9	0.6445	0.3402	0.2836	0.6053	0.1434	0.0709

as a 3D display device, but also as a traditional 2D display device.

D. THE MEASUREMENT OF THE COLOR GAMUT

In the prototype, traditional white LEDs backlight module is replaced by QD backlight. The QD backlight consists of blue LEDs and QDP film. Test images of pure blue, green, red and white color used in experiment are shown in Fig. 14(a)-Fig. 14(d) with detailed RGB information.

When measuring the color gamut, the device is in 2D mode. CA310 is used to measure the color coordinates of 9 measuring points, which are evenly distributed on the screen, as shown in Fig. 14(e). Two other commercial 3D displays (BENQ XL2707-B and View Sonic VX2268WM) are chosen as control group. In Table. 2, experiment results are presented; and in Fig. 15, photos of test images on those displays are presented. Same camera mentioned above (Nikon D3300, Exposure parameter: f/5.6, ISO-100, 1/60s) is used for shooting. Difference between photos might appear slight, but it still observable.

According to Rec.2020, the color gamut of those three displays are drawn in the CIE1931 chromaticity diagram and the results are shown in Fig. 16. Our stereoscopic prototype displays 77.98% color gamut, while BENQ XL2707-B and View Sonic VX2268WM achieve 55.69% and 54.37% repectively.

In terms of the reference white (D65) chromaticity coordinates (0.3127, 0.3290), the white coordinates of our prototype is (0.2612, 0.2497) and it remains tunable. The white coordinates of BENQ XL2707-B and View Sonic VX2268WM are (0.3077, 0.3215) and (0.3336, 0.3511).

The absolute photoluminescence quantum efficiency of the QD-polymer films, i.e. QDP down-conversion efficiency is about 80% (measured by a Horiba PTI Quanta Master 400). The concentration ratio between the red and green QD material is about 1:4. When the LCD panel displays different test images (As shown in Fig. 14(a)-Fig. 14(c)), the spectrums of our prototype are recorded in Fig. 17.

V. CONCLUSION

This paper introduces a wide color gamut autostereoscopic 2D-3D switchable display, which is based on eye tracking system and the application of dynamic subpixel arrangement method. Combined with the parallel computing method, this solution has further improved the real-time performance of our 3D display by reconstructing 3D images. And its use of Quantum-Dot material has greatly enhanced display quality. Based on the observation recorded, this 2D/3D switchable prototype clearly enjoys relative advantages in resolution, color gamut and crosstalk.

REFERENCES

[1] J. Geng, "Three-dimensional display technologies," *Adv. Opt. Photon.*, vol. 5, no. 4, pp. 456–535, Dec. 2013.

[2] S.-H. Lee, J.-M. Kim, and S.-W. Lee, "Behavioral circuit models of stereoscopic 3-D liquid crystal displays and shutter glasses," *IEEE Trans. Electron Devices*, vol. 62, no. 10, pp. 3302–3307, Oct. 2015.
[3] D. Park, T. G. Kim, and J. Cho, "A low-power time-synchronization processor with symmetric even/odd timer for charge-shared LCD driving of 3DTV active shutter glasses," *J. Display Technol.*, vol. 10, no. 12, pp. 1047–1054, Dec. 2014.
[4] F. Wu, G.-J. Lv, H. Deng, B.-C. Zhao, and Q.-H. Wang, "Dual-view integral imaging three-dimensional display using polarized glasses," *Appl. Opt.*, vol. 57, no. 6, pp. 1447–1449, Feb. 2018.
[5] R. Stefan and G. Raimund, "Use of linear and circular polarization: The secret LCD screen and 3D cinema," *Phys. Teacher*, vol. 55, no. 7, pp. 406–408, Oct. 2017.
[6] A. K. Srivastava, J. L. de Bougrenet de la Tocnaye, and L. Dupont, "Liquid crystal active glasses for 3D cinema," *J. Display Technol.*, vol. 6, no. 10, pp. 522–530, Oct. 2010.
[7] L. Shi, A. K. Srivastava, A. M. W. Tam, V. G. Chigrinov, and H. S. Kwok, "2D–3D switchable display based on a passive polymeric lenticular lens array and electrically suppressed ferroelectric liquid crystal," *Opt. Lett.*, vol. 42, no. 17, pp. 3435–3438, Sep. 2016.
[8] C. Kim, J. Kim, D. Shin, J. Lee, G. Koo, and Y. H. Won, "Electrowetting lenticular lens for a multi-view autostereoscopic 3D display," *IEEE Photon. Technol. Lett.*, vol. 28, no. 22, pp. 2479–2482, Nov. 15, 2016.
[9] C.-H. Chen, Y.-P. Huang, S.-C. Chuang, C.-L. Wu, H. P. D. Shieh, W. Mphepö, C.-T. Hsieh, and S. C. Hsu, "Liquid crystal panel for high efficiency barrier type autostereoscopic three-dimensional displays," *Appl. Opt.*, vol. 48, no. 18, pp. 3446–3454, Jun. 2014.
[10] Y. Meng, Z. Yu, C. Zhang, Y. Wang, Y. Liu, H. Ye, and L. L. Chen, "Numerical simulation and experimental verification of a dense multi-view full-resolution autostereoscopic 3D-display-based dynamic shutter parallax barrier," *Appl. Opt.*, vol. 58, no. 5, pp. 228–233, Feb. 2019.
[11] K.-H. Yoon, H. Ju, H. Kwon, I. Park, and S.-K. Kim, "Diffraction effects incorporated design of a parallax barrier for a high-density multi-view autostereoscopic 3D display," *Opt. Express*, vol. 24, no. 4, pp. 4057–4075, Feb. 2016.
[12] S. K. Yoon, S. Khym, H.-W. Kim, and S.-K. Kim, "Variable parallax barrier spacing in autostereoscopic displays," *Opt. Commun.*, vol. 370, no. 1, pp. 319–326 Jul. 2016.
[13] W. Mphepo, Y. P. Huang, and H. P. D. Shieh, "Enhancing the brightness of parallax barrier based 3D flat panel mobile displays without compromising power consumption," *J. Display Technol.*, vol. 6, no. 2, pp. 60–64, Feb. 2010.
[14] Z. Zhuang, L. Zhang, P. Surman, W. Song, S. Thibault, X. W. Sun, and Y. Zheng, "Addressable spatial light modulators for eye-tracking autostereoscopic three-dimensional display using a scanning laser," *Appl. Opt.*, vol. 57, no. 16, pp. 4457–4466, Jun. 2018.
[15] Y. S. Hwang, F.-K. Bruder, T. Fäcke, S.-C. Kim, G. Walze, R. Hagen, and E.-S. Kim, "Time-sequential autostereoscopic 3-D display with a novel directional backlight system based on volume-holographic optical elements," *Opt. Express*, vol. 22, no. 8, pp. 9820–9838, Apr. 2014.
[16] Z. Zhuang, L. Zhang, P. Surman, S. Guo, B. Cao, Y. Zheng, and X. W. Sun, "Directional view method for a time-sequential autostereoscopic display with full resolution," *Appl. Opt.*, vol. 55, no. 28, pp. 7847–7854 Oct. 2016.
[17] J.-L. Feng, Y.-J. Wang, S.-Y. Liu, D.-C. Hu, and J.-G. Lu, "Three-dimensional display with directional beam splitter array," *Opt. Express*, vol. 25, no. 2, pp. 1564–1572, Jan. 2017.
[18] Z. Luo, D. Xu, and S.-T. Wu, "Emerging quantum-dots-enhanced LCDs," *J. Display Technol.*, vol. 10, no. 7, pp. 526–539, Jul. 2014.
[19] T. Xuan, J. Huang, H. Liu, S. Lou, L. Cao, W. Gan, R.-S. Liu, and J. Wang, "Super-hydrophobic cesium lead halide perovskite quantum dot-polymer composites with high stability and luminescent efficiency for wide color gamut white light-emitting diodes," *Chem. Mater.*, vol. 31, no. 3, pp. 1042–1047, Feb. 2019.
[20] H.-W. Chen, R.-D. Zhu, J. He, W. Duan, W. Hu, Y.-Q. Lu, M.-C. Li, S.-L. Lee, Y.-J. Dong, and S.-T. Wu, "Going beyond the limit of an LCD's color gamut," *Light, Sci. Appl.*, vol. 6, no. 5, Sep. 2017, Art. no. e17043.
[21] L. Luo, Q.-H. Wang, H. Deng, H. Ren, S. Li, and Y. Xing, "360-degree viewable tabletop 3D display system based on integral imaging by using perspective-oriented layer," *Opt. Commun.*, vol. 438, no. 5, pp. 54–60, May 2019.
[22] L. Yang, X. Sang, X. Yu, B. Yan, K. Wang, and C. Yu, "Viewing-angle and viewing-resolution enhanced integral imaging based on time-multiplexed lens stitching," *Opt. Express*, vol. 27, no. 11, pp. 15679–15692, May 2019.
[23] B. Chen, L. Ruan, and M.-L. Lam, "Light field display with ellipsoidal mirror array and single projector," *Opt. Express*, vol. 27, no. 15, pp. 21999–22016, Jul. 2019.
[24] X. Yu, X. Sang, X. Gao, D. Chen, B. Liu, L. Liu, C. Gao, and P. Wang, "Dynamic three-dimensional light-field display with large viewing angle based on compound lenticular lens array and multi-projectors," *Opt. Express*, vol. 27, no. 11, pp. 16024–16031, May 2019.
[25] Y. Su, Z. Cai, L. Shi, F. Zhou, H. Chen, J. Wu, and K. Wu, "Projection-type multiview holographic three-dimensional display using a single spatial light modulator and a directional diffractive device," *IEEE Photon. J.*, vol. 10, no. 5, Oct. 2018, Art. no. 7000512.
[26] J. Park, K. Lee, and Y. Park, "Ultrathin wide-angle large-area digital 3D holographic display using a non-periodic photon sieve," *Nature Commun.*, vol. 10, no. 5, Mar. 2019, Art. no. 1304.
[27] H.-L. Zhang, H. Deng, J.-J. Li, M.-Y. He, D.-H. Li, and Q.-H. Wang, "Integral imaging-based 2D/3D convertible display system by using holographic optical element and polymer dispersed liquid crystal," *Opt. Lett.*, vol. 44, no. 2, pp. 387–390, Jan. 2019.
[28] G. Chidichimo, A. Beneduci. V. Maltese, S. Cospito, A. Tursi, P. Tassini, and G. Pandolfi, "2D/3D switchable displays through PDLC reverse mode parallax barrier," *Liq. Cryst.*, vol. 45, no. 13, pp. 2132–2138, Jul. 2018.
[29] A. J. Woods, "Crosstalk in stereoscopic displays: A review," *J. Electron. Imag.*, vol. 21, no. 4, Oct. 2012, Art. no. 040902.
[30] H. Fan, Y. Zhou, J. Wang, H. Liang, P. Krebs, J. Su, D. Lin, K. Li, and J. Zhou, "Full resolution, low crosstalk, and wide viewing angle autostereoscopic display with a hybrid spatial-temporal control using free-form surface backlight unit," *J. Display Technol.*, vol. 11, no. 7, pp. 620–624, Jul. 2015.
[31] H. W. Liang, S. An, J. Wang, Y. Zhou, H. Fan, P. Krebs, and J. Zhou, "Optimizing time-multiplexing auto-stereoscopic displays with a genetic algorithm," *J. Display Technol.*, vol. 10, no. 8, pp. 695–699, Aug. 2014.

BIN XU was born in Shandong, China, in 1989. He received the master's degree from the Stereo Imaging Technology (SIT) Laboratory, Nanjing University, China, where he is currently pursuing the Ph.D. degree in electrical circuit and systems.

His research interests include autostereoscopic displays, and optical and electrical technology.

XUELING LI was born in Jilin, China, in 1996. She received the B.Sc. degree in electronic information science and technology from Nanjing University, China, in 2018, and the master's degree from the Stereo Imaging Technology (SIT) Laboratory, Nanjing University, where she is currently pursuing the Ph.D. degree in electrical circuit and systems.

Her research interests include autostereoscopic displays, and optical and electrical technology.

YUANQING WANG received the B.S. and M.S. degrees from Zhejiang University and the Ph.D. degree from Nanjing University. He is currently a Professor with the School of Electronic Science and Engineering, Nanjing University. He was involved in the research work on optical electrical imaging and measuring systems, and special display technologies. He has completed various research projects, such as the National Hi-tech Research and Development Plan (863 Plan) of China, the National Natural Science Foundation of China, Jiangsu Hi-tech Plan, and so on. His current research interests include optical electronics and information processing, especially in LIDAR and 3D display. He is the Chairman of the 3D Imaging and Display Committee, China, and the IEC International Standard Workgroup Experts in Display Technology.